

## Simulations of unstable recollimation shocks

---

**Agnese Costa,<sup>a,b,\*</sup> Gianluigi Bodo,<sup>c</sup> Fabrizio Tavecchio<sup>b</sup> and Paola Rossi<sup>c</sup>**

<sup>a</sup>*DiSAT, Università dell'Insubria, Via Valleggio 11, I-22100 Como, Italy*

<sup>b</sup>*INAF – Osservatorio Astronomico di Brera, via E. Bianchi 46, 23807 Merate, Italy*

<sup>c</sup>*INAF – Osservatorio Astrofisico di Torino, Strada Osservatorio 20, 10025 Pino Torinese, Italy*

*E-mail: [agnese.costa@inaf.it](mailto:agnese.costa@inaf.it)*

3D relativistic (magneto)hydrodynamical simulations of the confinement of jets revealed that the jet-environment interface downstream of recollimation shocks is susceptible to instabilities that can be strong enough to destroy the jet structure and quickly decelerate it to sub-relativistic velocities. This is in contrast with the picture, supported by 2D, of confined jets undergoing a series of recollimation and reflection shocks. Motivated by the impact of such a different scenario on the evolution and radiation of jetted active galactic nuclei (AGNs), we investigate the stability of relativistic AGN jets at recollimation, by means of high resolution 3D hydrodynamical simulations, devoted to unveil the interplay among the various instabilities developing. In this work we show the results for a low-power unstable jet, compatible with the properties of Fanaroff-Riley type 0 radio-galaxies. We suggest that the differences between high- and low-power radio-galaxies, as well as differences among high-energy peaked blazars, could be interpreted as a transition between stable and unstable configurations.

*High Energy Phenomena in Relativistic Outflows VIII (HEPROVIII)*

*23-26 October, 2023*

*Paris, France*

---

\*Speaker

## 1. Introduction

Relativistic jets expelled by active galactic nuclei (AGNs) are among the most powerful sources in the Universe. They emit intense radiation across the whole electromagnetic spectrum, up to very high energies, and largely contribute to the cosmic ray background. Consequently, understanding the dynamics and radiation of AGN jets is a crucial endeavor, complicated by their diverse nature and by the strong interplay between processes taking place at length-scales different by many orders of magnitude. Unanswered questions revolve around the composition of the jet plasma, the mechanisms governing emission and particle acceleration and the very launching process and inner jet structure [e.g. 1]. In particular, great effort has been dedicated to investigate the stability and confinement of jets: in light of the variety of instabilities that can influence their dynamics, such as Kelvin-Helmholtz (KHI), centrifugal (CFI), and Rayleigh-Taylor (RTI) [e.g. 2–4], it is remarkable that jets can propagate to extraordinary distances, even reaching  $10^9$  times their initial radius. Indeed, it has often been suggested that the different properties of low-power and high-power jets, classified as Fanaroff-Riley I (FRI) and Fanaroff-Riley II (FR II) sources [5], can be attributed to instabilities and the resulting entrainment of external gas [6, 7].

Recent research has emphasized the crucial role of the region downstream of recollimation shocks in promoting the growth of instabilities at the jet-environment contact discontinuity (CD). When confined by an external medium, jets are known to undergo a series of recollimation and reflection shocks [8, 9], as confirmed by axisymmetric 2D simulations [10]. However, 3D simulations have revealed that the downstream of curved shocks is subject to a combination of KHI, CFI, RTI, and Richtmyer-Meshkov instability (RMI) [3, 11, 12]. It's noteworthy that intense toroidal magnetic fields have been shown to suppress the recollimation instabilities [13], but in the case of low-magnetized jets these can be powerful enough to disrupt the jet spine through strong turbulence. This calls for a survey of the stability of recollimation shocks in astrophysical jets; in particular we focus on AGN jets. Here we present our results for a sample case of a low-power, unstable jet.

## 2. Simulation setup

### 2.1 The problem

We investigate the stability of a relativistic jet in a stratified external medium by means of numerical simulations. We consider an initially conical jet [as in 9] at a distance  $z \in [z_0, z_{max}]$  from its cone vertex, that is moving relativistically through an external medium at rest, whose pressure and density are characterized by power-law profiles of index  $\eta$ :  $\rho_{ext}(z) = \rho_{ext}(z_0) (z/z_0)^{-\eta}$  and  $p_{ext}(z) = p_{ext}(z_0) (z/z_0)^{-\eta}$ . The environment is isothermal, with temperature  $\mathcal{T}_{ext} = \frac{p_{ext}(z_0)}{\rho_{ext}(z_0)c^2}$ . The jet's steady state is completely determined by the Lorentz factor  $\Gamma_j$ , the jet-environment density and pressure contrast at the jet base  $\nu = \frac{\rho_j(z_0)}{\rho_{ext}(z_0)}$ ,  $P_r = \frac{p_j(z_0)}{p_{ext}(z_0)}$ , and the initial opening angle  $\theta_j$ . As the jet expands, its density and pressure decay adiabatically and if  $\eta < 2$  the external pressure can confine the jet through a recollimation shock [14], that would start the series of recollimation-reflection shocks in the axisymmetric picture.

We show here the outcome of a 3D relativistic hydrodynamical (RHD) simulation of a mildly relativistic, light and cold jet, in a cold confining environment: we set

$$\Gamma_j = 5, \quad \nu = 7.6 \times 10^{-6}, \quad P_r = 10^{-3}, \quad \theta_j = 0.2, \quad \eta = 0.5, \quad \mathcal{T}_{ext} = 3 \times 10^{-6}. \quad (1)$$

## 2.2 Numerical implementation

Simulations are performed with the RHD module of the PLUTO [15] code, that solves the set of relativistic hydrodynamics equations, which in the observer's frame are

$$\frac{\partial}{\partial t} \begin{pmatrix} \rho\Gamma \\ \rho h\Gamma^2 \mathbf{v} \\ \rho h\Gamma^2 - p \\ \rho\Gamma f \end{pmatrix} + \nabla \cdot \begin{pmatrix} \rho\Gamma \mathbf{v} \\ \rho h\Gamma^2 \mathbf{v}\mathbf{v} + p\mathbf{I} \\ \rho h\Gamma^2 \mathbf{v} \\ \rho\Gamma f \mathbf{v} \end{pmatrix} = \begin{pmatrix} 0 \\ \mathbf{f}_g \\ \mathbf{f}_g \cdot \mathbf{v} \\ 0 \end{pmatrix}. \quad (2)$$

$\rho$ ,  $\Gamma$ ,  $h$ ,  $\mathbf{v}$ ,  $p$ , respectively denote the rest-frame number density, the Lorentz factor, the proper specific enthalpy, the 3-velocity in units of  $c$ , and the fluid pressure, while  $\mathbf{f}_g$  is the specific external force that sustains dynamical equilibrium in the environment. We define it as  $\mathbf{f}_g(z) = \nabla p_{ext}(z)$ . We also evolve a passive tracer  $f$ , initially set to 1 for the injected relativistic jet, and to 0 for the external gas. The system is closed by defining the equation of state (EoS) as  $h = \frac{5}{2}\mathcal{T} + \sqrt{\frac{9}{4}\mathcal{T}^2 + 1}$ , where  $\mathcal{T} = p/(\rho c^2)$ , that approximates the Sygne EoS of a single-species relativistic perfect fluid.

Since our aim is to study the stability of the jet downstream of the recollimation shock, we adopted the following procedure: we performed a 2D simulation until steady state, which we then used as initial condition in a 3D simulation. All the details of our approach are described in [16]. The 2D simulation is carried out in cylindrical coordinates  $\{r, z\} \in [0, 20] \times [0.5, 30]$  in units of  $z_0$ , with the initial condition described above. We include a region  $z \in [0.5, 1]$  where we fix the jet injection, and we add a shear at the CD for avoiding numerical artifacts [11, 16]. Starting from the 2D steady state, the 3D simulation uses Cartesian coordinates  $\{x, y, z\} \in [-5, 5] \times [-5, 5] \times [1, 30]$ . We ran it until a quasi steady state was reached. We adopted outflow boundary conditions everywhere, except at  $z_0$ , where we fix the initial conditions, and at the jet axis in the 2D simulation, where we use an appropriate reflective prescription. We employed a linear reconstruction scheme, a second order Runge-Kutta method for time integration, and the HLLC Riemann solver of PLUTO.

## 3. Results

Once we relax the axisymmetry constraint in the 3D simulation, the 2D steady state results highly unstable. The overall dynamics of the series of recollimation-reflection shocks undergoes significant modifications, resulting in a 3D quasi-stationary state characterized by entrainment and, consequently, deceleration of the jet. Fig. 1 shows the jet structure through a volume rendering of the  $z$  component of the 4-velocity,  $\Gamma v_z$ , at the end of the 3D simulation. At first the jet is relativistic, with  $\Gamma v_z > 3$  (yellow-red), and two distinct confinement stages can be observed. Later on, external gas is entrained and the spreading of momentum results in a transition to sub-relativistic speeds ( $\Gamma v_z \leq 1$ , light blue). The nature of the instability appears to be a combination of KHI, CFI, and RMI, with signs of KHI-induced helical deformations in Fig. 1. Fig. 2 better displays the effect of the growth of the recollimation-reflection instabilities on the jet dynamics. Fig. 2 shows in a unique figure the maps of the tracer of entrained material (left) and the Lorentz factor (right) in the  $y = 0$  plane. On the left, the stationary axisymmetric jet profile is superimposed in white, while on the right the four horizontal white lines pinpoint the positions of the  $z = z^*$  planes showcased in Fig. 3, which exhibits the development of the instability through 4 maps of the 4-velocity  $\Gamma v_z$ .

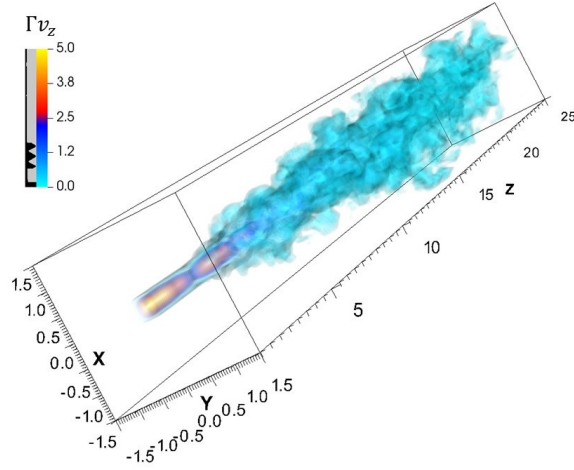


**Figure 1:** 3D visualization of the jet propagation 4-velocity  $\Gamma v_z$ . The accompanying black-grey bar illustrates the transparency levels, denoting which values of  $\Gamma v_z$  appear opaque (grey) or transparent (black).

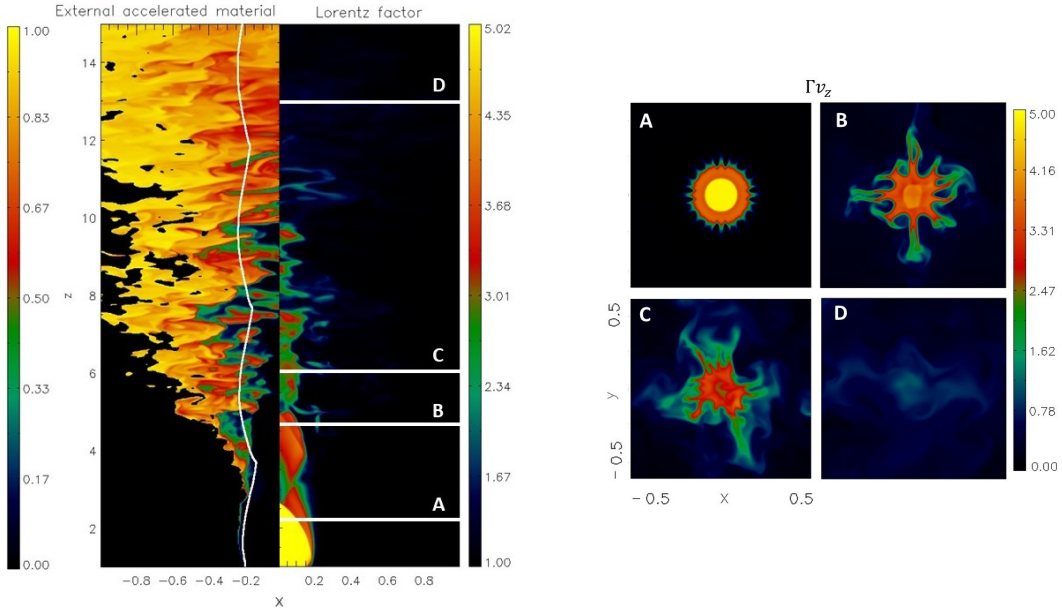


**Figure 2:** Maps of the Lorentz factor (right) and the tracer of the entrained external gas (left), selected through the propagation velocity,  $v_z \geq 0.1$ , at  $y = 0$  in the  $x - z$  plane. We over-plotted the contour of the axisymmetric 2D steady state jet on the left.

**Figure 3:** Maps of the 4-velocity  $\Gamma v_z$  at 4 different altitudes  $z^* = [2.3, 4.7, 6.1, 13]$  indicated by the horizontal lines in Fig. 2.

The first recollimation shock (yellow-orange boundary in Fig. 2 and 3A) reaches the axis at  $z \approx 2.6$ , where a reflection shock starts expanding: the jet downstream the oblique shock is decelerated but still is relativistic, with  $\Gamma \approx 3.5$ , and the deflected streamlines converge at the recollimation point supersonically. Downstream the recollimation shock, the pressure of the jet equals the outside pressure; then as it increases after the reflection shock, it drives an expansion, until pressure equilibrium is reached again at the antinode,  $z \approx 3.8$ . During this phase, external

material starts to be entrained (as seen on the left of 2), as a result of perturbations induced by the CFI and the KHI growing at the CD. Near the antinode, the RMI is also triggered where the reflection shock crosses the CD, corrugated by the KHI and CFI [12], with finger-like structures typical of the RTI, CFI and RMI visible in Fig. 3B. After the antinode the jet is confined and decelerated again through a second recollimation shock, but its downstream is not fast enough to cause another reflection shock, and only a mildly relativistic spine survives (Fig. 3C) until  $z \simeq 10 - 12$ . The jet is heavily entraining external material; as its momentum is distributed to the heavier gas, its velocity decreases to become completely sub-relativistic at larger distances (Fig. 3D). The thermal energy of the jet will increase in the regions with higher pressure, especially downstream of the reflection shock, and we expect that part of the bulk kinetic energy of the jet will be dissipated through radiation.

#### 4. Final remarks

As mentioned in the Introduction, the distinction between jetted AGNs could partially be ascribed to large scale instabilities, able to efficiently decelerate jets, while entraining external material. The effect of instabilities seems to be especially relevant at the lower jet powers, for FRI sources [3], and especially for the FRO subclass of radio-galaxies [16]: the shortest, weakest, and most common [17, for a review]. If we set the density and length scales of the simulation to  $z_0 = 1$  pc, and  $\rho_{ext}(z_0) = 1 m_p \text{ cm}^{-3}$ , where  $m_p$  is the proton mass, the simulated jet has power

$$L_j = \pi(z_0\theta_j)^2 v_z \left( \rho_j c^2 h_j \Gamma^2 \right) \simeq 10^{40} \left( \frac{\rho_{ext}(z_0)}{1 m_p \text{ cm}^{-3}} \right) \left( \frac{z_0}{1 \text{ pc}} \right)^2 \text{ erg s}^{-1}, \quad (3)$$

suitable to describe such low-power jets. In this scenario the jet emits the most downstream of the reflection shock, creating a bright spot that would correspond to the parsec scale core observed in FROs. For blazars, it was shown [18, 19] that the concurrence of turbulence and strong shocks can be a viable mechanism for explaining the peculiar high-energy emission bump of TeV blazars. Within this framework, the difference between high energy peaked blazars (HBL) and the more extreme TeV blazars may reflect a distinction between stable and unstable jets. Different values of the parameters described in Section 2.2 can trigger different recollimation instabilities, leading to jets that are more or less stable, depending on the Lorentz factor, temperature, opening angle and overall luminosity. A comprehensive parameter study will be pursued in a forthcoming paper (Costa et al. in prep.). Finally, incorporating magnetic fields in our simulations will be instrumental and potentially decisive for confirming or ruling out such scenarios since they can considerably change the evolution of instabilities.

#### References

- [1] R. Blandford, D. Meier and A. Readhead, *Relativistic Jets from Active Galactic Nuclei*, *ARA&A* **57** (2019) 467 [1812.06025].
- [2] G. Bodo, G. Mamatsashvili, P. Rossi and A. Mignone, *Linear stability analysis of magnetized relativistic rotating jets*, *MNRAS* **485** (2019) 2909 [1902.10781].

- [3] K.N. Gourgouliatos and S.S. Komissarov, *Reconfinement and loss of stability in jets from active galactic nuclei*, *Nature Astronomy* **2** (2018) 167 [1806.05683].
- [4] J. Matsumoto and Y. Masada, *Propagation, cocoon formation, and resultant destabilization of relativistic jets*, *MNRAS* **490** (2019) 4271 [1910.11578].
- [5] B.L. Fanaroff and J.M. Riley, *The morphology of extragalactic radio sources of high and low luminosity*, *MNRAS* **167** (1974) 31P.
- [6] M. Perucho, J.M. Martí, R.A. Laing and P.E. Hardee, *On the deceleration of Fanaroff-Riley Class I jets: mass loading by stellar winds*, *MNRAS* **441** (2014) 1488 [1404.1209].
- [7] P. Rossi, G. Bodo, S. Massaglia and A. Capetti, *The different flavors of extragalactic jets: The role of relativistic flow deceleration*, *A&A* **642** (2020) A69 [2007.11423].
- [8] S.S. Komissarov and S.A.E.G. Falle, *Simulations of Superluminal Radio Sources*, *MNRAS* **288** (1997) 833.
- [9] G. Bodo and F. Tavecchio, *Recollimation shocks and radiative losses in extragalactic relativistic jets*, *A&A* **609** (2018) A122 [1710.06713].
- [10] Y. Mizuno, J.L. Gómez, K.-I. Nishikawa, A. Meli, P.E. Hardee and L. Rezzolla, *Recollimation Shocks in Magnetized Relativistic Jets*, *ApJ* **809** (2015) 38 [1505.00933].
- [11] P. Abolmasov and O. Bromberg, *Interface instabilities in hydrodynamic relativistic jets*, *MNRAS* **520** (2023) 3009 [2210.11178].
- [12] J. Matsumoto and Y. Masada, *Two-dimensional Numerical Study for Rayleigh-Taylor and Richtmyer-Meshkov Instabilities in Relativistic Jets*, *ApJ* **772** (2013) L1 [1306.1046].
- [13] J. Matsumoto, S.S. Komissarov and K.N. Gourgouliatos, *Magnetic inhibition of the recollimation instability in relativistic jets*, *MNRAS* **503** (2021) 4918 [2010.11012].
- [14] O. Porth and S.S. Komissarov, *Causality and stability of cosmic jets*, *MNRAS* **452** (2015) 1089 [1408.3318].
- [15] A. Mignone, G. Bodo, S. Massaglia, T. Matsakos, O. Tesileanu, C. Zanni et al., *PLUTO: a Numerical Code for Computational Astrophysics*, in *JENAM-2007, “Our Non-Stable Universe”*, pp. 96–96, Aug., 2007.
- [16] A. Costa, G. Bodo, F. Tavecchio, P. Rossi, A. Capetti, S. Massaglia et al., *FRO jets and recollimation-induced instabilities*, *A&A* **682** (2024) L19.
- [17] R.D. Baldi, *The nature of compact radio sources: the case of FR 0 radio galaxies*, *A&A Rev.* **31** (2023) 3 [2307.08379].
- [18] F. Tavecchio, A. Costa and A. Sciacaluga, *Extreme blazars: the result of unstable recollimated jets?*, *MNRAS* **517** (2022) L16 [2207.12766].
- [19] A. Sciacaluga and F. Tavecchio, *Extreme TeV BL Lacs: a self-consistent stochastic acceleration model*, *MNRAS* **517** (2022) 2502 [2208.00699].